

[SUPPLEMENTARY MATERIAL]

Animating matter

A material-led exploration into the kinetic potential of nylon monofilament

Ana Inés Piñeyro Irazábal | Royal College of Art | September 2019

Contents

S.1. Tuning of mandrel coils	1
S.1.1. Twist insertion and coiling over the mandrel.....	1
S.1.2. Heat setting of the coiled shape	4
S.1.3. Thermally-induced activation and shape recovery after activation.....	11
S.2. Tuning of twisted mandrel coils	17
S.2.1. Twist insertion and locking of the folded structure.....	17
S.2.2. Training of twisted mandrel coils.....	21
S.2.3. Heat-responsive kinetic capacity of twisted mandrel coils.....	22
References	29

S.1. Tuning of mandrel coils

This section describes the identification of suitable parameter values for the formation of mandrel coils (MCs), leading to the formalisation of the process under the working set-up used in this research.

MCs are formed by inserting twist into the monofilament to a point just before a coil starts forming, subsequently winding the high twist monofilament over a mandrel (or metal rod), and heat setting the coiled structure before removing it from the mandrel (Haines *et al.*, 2014ab).

S.1.1. Twist insertion and coiling over the mandrel

I used the vertical set-up described in Figure 3 (main text) to insert twist into the monofilament. I employed screw clamps, as the ones found inside the plastic cover of electrical terminal blocks, to fasten the monofilament to the mandrel, and fitted tubular metallic crimp tubes (2mm diameter) to both ends of the monofilament to make it easier to clamp it (Figure S.1). During twist-insertion, I used the mandrel to hold the weight needed to apply an appropriate tension to the monofilament. I wound the high twist monofilament over the mandrel while it was still hanging from the twist-insertion device.

S.1.1.1. Relevant formation parameters

Through the intuitive exploration, the literature review and the process of translation I have identified the following parameters that intervene in the formation of MCs (Table 17, main text):

- mandrel diameter;
- twisting and winding directions;
- weight used during twisting and winding;
- twist density in the monofilament prior to winding it over the mandrel;
- coil pitch during winding (i.e., distance between consecutive monofilament turns over the mandrel);
- heat setting temperature;
- heat setting exposure time;
- activation temperature during training;
- number of training cycles.



Figure S.1. Screw clamps and mandrel (top row, left). Crimp tubes attached to the monofilament (top row, right). Monofilament fastened to a mandrel with a screw clamp (middle row). Monofilament wound over a mandrel and fastened with screw clamps (bottom row).

Twisting and winding directions

As described in Chapter 3 of the main text, the relation between the twisting and winding directions determines the heat-responsive behaviour of MCs: i.e., homochiral coils, where the twisting and winding directions match, contract in response to heat, whereas heterochiral coils, where the twisting and winding directions are opposite, expand in response to heat (Haines *et al.*, 2014ab). Both types of coils were formed during this exploration.

Mandrel diameter

As part of the formalisation of formation processes (Chapter 7 and Appendix B of the main text), this exploration was bounded by the use of one single type of monofilament (0.45mm-diameter Skysper fishing line) and one mandrel diameter (3mm). Coils formed with this material and tool present spring indices¹ of approximately 7.3, providing a clear distinction regarding TICs, whose spring indices may range between 1.1 and 1.7 (Haines *et al.*, 2014ab).

Twisting and winding weight

I tested weights between 40g and 190g to set the monofilament in tension while twisting it and winding it over the mandrel. These weights did not show any influence on the structure or the behaviour of the coils. The MCs described in this section were formed using 40g both during twisting and winding.

The subsequent exploration carried out on the effects of the force used to wind C-TICs on their structure (Appendix B, section B.4.3 of the main text), suggests that the weight range tested for MCs might be too low to render variations in their structure. It is possible that larger weights may lead to the emergence of a helical overall contour in MCs, similar to the one observed in sample 4 (Figure 28.A., main text), and this should be further explored.

Number of turns inserted into the monofilament prior to winding

When twisting the monofilament under 40g the coil starts forming at around 480t/m. In order to avoid the formation of the coil while obtaining a monofilament with a high twist that would be subsequently wound over the mandrel, I used 450t/m.

Coil pitch

Given that this research suggests the activation of monofilament morphologies from relaxed, non-stretched nor compressed states, the amplitude of the shape change performed by homochiral MCs can be maximised by increasing the distance between adjacent coil rings, allowing these to come closer to each other during thermally-induced contraction. On the

¹ The spring index of a coil is the ratio between the mean coil diameter and the monofilament diameter. The mean coil diameter is given by the outer diameter of the coil minus the diameter of the monofilament. Outer diameters of the coils obtained by winding a 0.45mm-diameter monofilament around a 3mm-diameter mandrel ranged between 3.7mm and 3.8mm.

other hand, the amplitude of the shape change performed by heterochiral MCs can be maximised when these present contiguous rings, increasing the distance that adjacent rings may gain between them during thermally-induced expansion. Hence, I intended to form homochiral MCs with long pitch and heterochiral MCs with contiguous rings.

The pitch of a MC can be determined when laying the monofilament around the mandrel, by determining the separation between consecutive turns. While I have not implemented a consistent way of obtaining an even pitch when winding the monofilament around the mandrel, I found that different pitch may result in MCs from the heat setting process, as it is described in the next section.

S.1.2. Heat setting of the coiled shape

The temperature and duration of the exposure of a MC to heat that is required to lock the coiled shape depend on the composition of the monofilament. Coils can be heat set “above the maximum actuation temperature, but below the polymer melting point” (Haines *et al.*, 2014b). Given that the type of nylon which the Skysper monofilament is made from is not known, I took the melting points for nylon 6 and nylon 6.6 as reference values for the heat-setting tests.²

Using a halogen oven (Figure 36, main text), I tested the heat setting of coils from Skysper monofilament under temperatures between 90°C and 215°C and exposure times between 2 minutes and 1 hour. I evaluated the resulting structures by observing:

- the appearance of the monofilament: its colour;
- the structure of the coil: the degree to which the coiled shape was formed, the coil pitch and the length of the coil;
- the orientation of coil rings when the coil was stretched;
- the variation of coil pitch over time (denoted by a change of length in the coil).

I considered samples appropriately heat set when coil rings did not skew when I stretched the coils (e.g., Figure S2), and when the pitch, and consequently the length of the coil,

² Typical melting points for nylon 6 are 220-260°C, and for nylon 6.6 257-270°C (Wypych 2016; p.216,222).

remained stable over time. I favoured samples where the colour of the monofilament did not change or showed the smallest change after being heat set.



Figure S2. Mandrel coil: rings skew when the coil is stretched.

The temperature values given in this section refer to the temperature set in the oven for each trial.³ I pre-heated the oven at the maximum temperature available (250°C), changing it to the heat-setting temperature once the samples were placed inside the oven.⁴

At 90°C with an exposure time of 60 minutes, homochiral coils resulted with contiguous rings and these skewed when the coil was stretched. Heterochiral coils presented a long pitch (i.e., long distance between adjacent rings) and its rings did not skew when the coil was stretched. The appearance of the monofilament was not changed (Figure S3). 24 hours after removing the coils from the mandrel, the length of the homochiral coil had decreased by 22%, and the length of the heterochiral coil had increased by 260%.

When heat set at 150°C with an exposure of 10 minutes, the homochiral coil resulted with contiguous rings and these slightly skewed at the ends of the coil when it was stretched. The heterochiral coil showed inter-ring distance and rings did not skew when the coil was stretched. The appearance of the monofilament was not changed (Figure S4). 24 hours after being removed from the mandrel, the length of the homochiral coil remained almost constant and the heterochiral coil got considerably longer, increasing approximately 280% in length.

³ The temperature inside the oven varies along both the vertical and horizontal directions. In order to obtain coils that were evenly set along their length, I resorted to form coils that were shorter than approximately 5cm, heat setting them one at a time, so that they could be placed always in the same location inside the oven, providing temperatures as similar as possible to each coil.

⁴ Pre-heating the oven to a higher temperature than the one being tested, allowed me to overcome the temperature drop that takes place when opening the lid of the oven to place the mandrels inside. Controlling the interval during which I kept the door of the oven open while introducing the mandrel, allowed me to decrease the variation of the temperature across heat-setting instances.

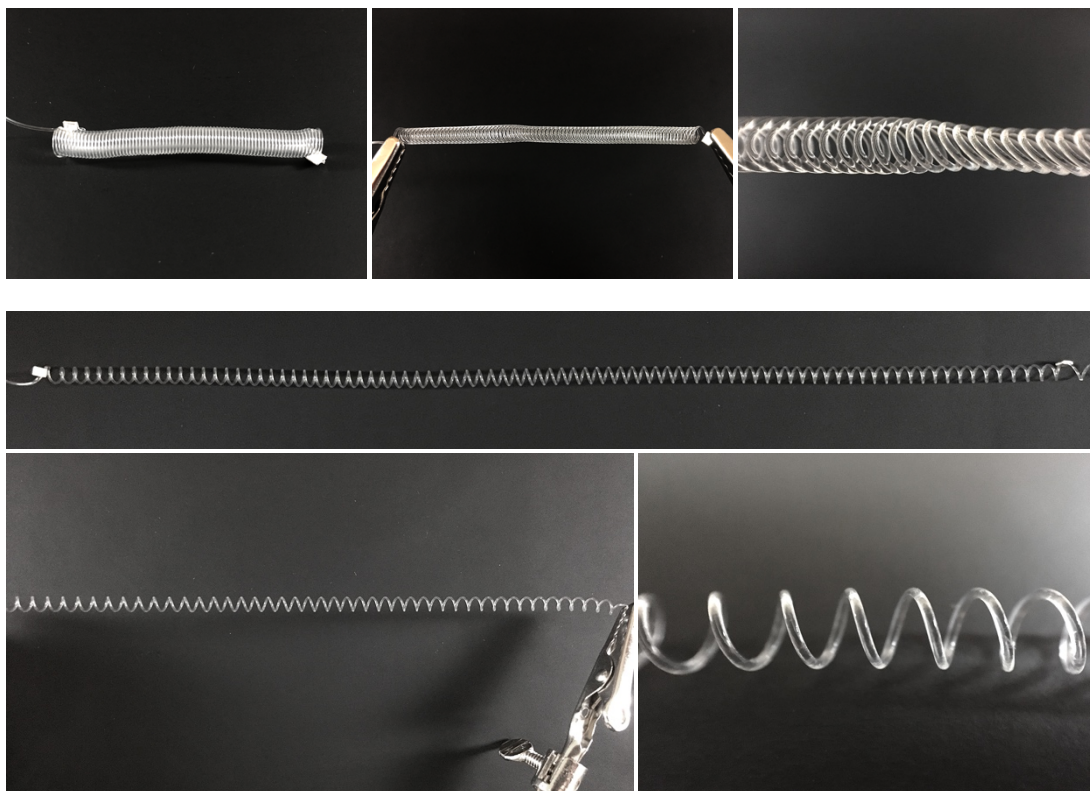


Figure S3. Mandrel coils heat set at 90°C for 60 minutes. Homochiral coil (top): full coil (left), stretched coil (centre) and detail of stretched coil (right). Heterochiral coil (bottom): full coil (top row); stretched coil (bottom row, left) and detail of relaxed coil (bottom row, right).

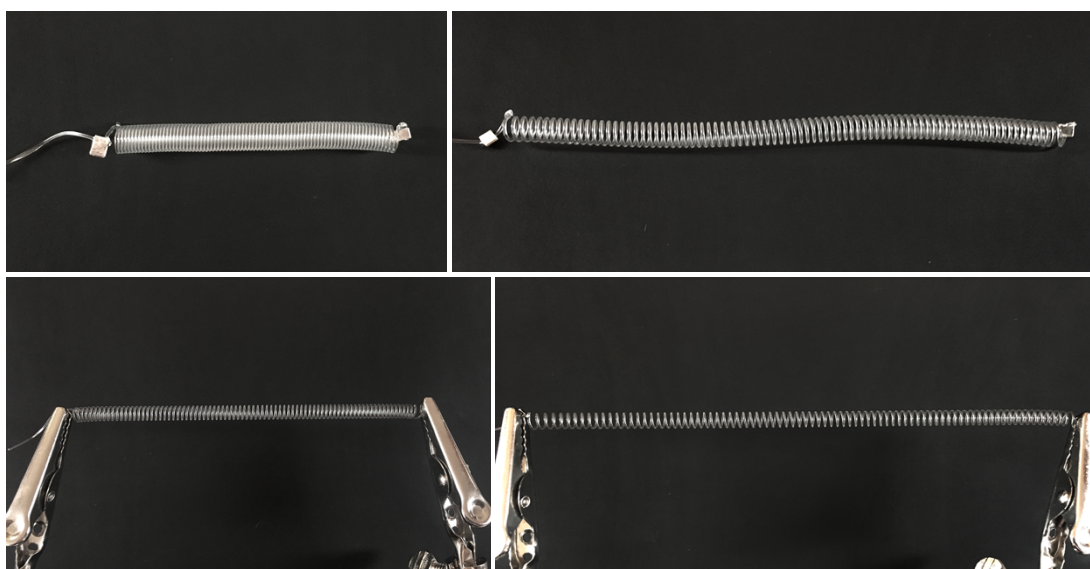


Figure S4. Homochiral (left) and heterochiral (right) mandrel coils heat set at 150°C for 10 minutes. Relaxed coil (top row) and stretched coil (bottom row).

At 150°C, over a 60-minute exposure, the homochiral coil resulted also with contiguous rings, and the heterochiral coil presented separation between consecutive rings, but the sample was shorter than the coil that was heat set for 10 minutes under the same temperature. The rings of neither sample skewed when stretched, and the monofilament acquired a yellow tint

(Figure S5). After 24 hours of being removed from the mandrel, the length of the homochiral coil remained almost constant, and that of the heterochiral coil increased by approximately 293%.

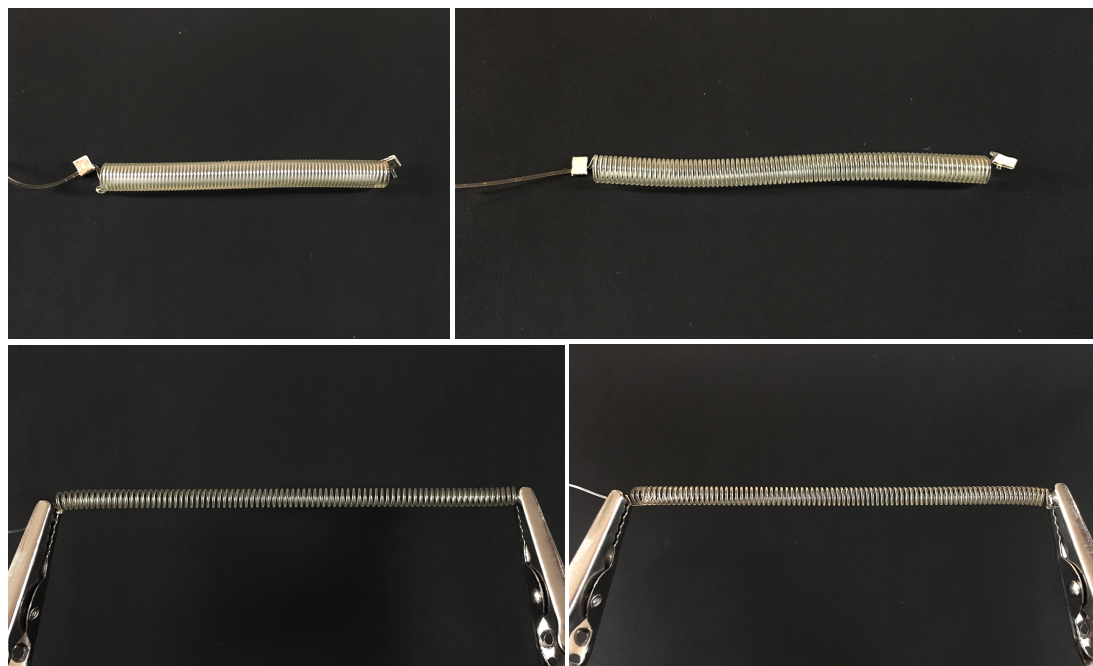


Figure S5. Homochiral (left) and heterochiral (right) mandrel coils heat set at 150°C for 60 minutes. Relaxed coil (top row) and stretched coil (bottom row).

At 200°C with exposures of 3 and 4 minutes, homochiral coils resulted with separation between adjacent rings, while heterochiral ones resulted with contiguous rings, reverting the tendency observed under the previous heat-setting values. The homochiral coil heat set for 4 minutes was longer than the one heat set for 3 minutes, presenting a longer separation between consecutive rings. Coils resulting from both exposure times did not skew when stretched. While the appearance of the monofilament was not affected in exposures of 3 minutes, it acquired a yellow tone in exposures of 4 minutes (Figure S6 and Figure S7, respectively). The length of the heterochiral coils for the two exposure times remained almost constant after 24 hours from removing the samples from the mandrel, while the length of the homochiral coils changed, but in opposite directions: the homochiral coil heat set for 3 minutes got shorter over time, with a length decrease of approximately 10.8%; whereas the one heat set for 4 minutes got slightly longer, increasing approximately 138% in length.

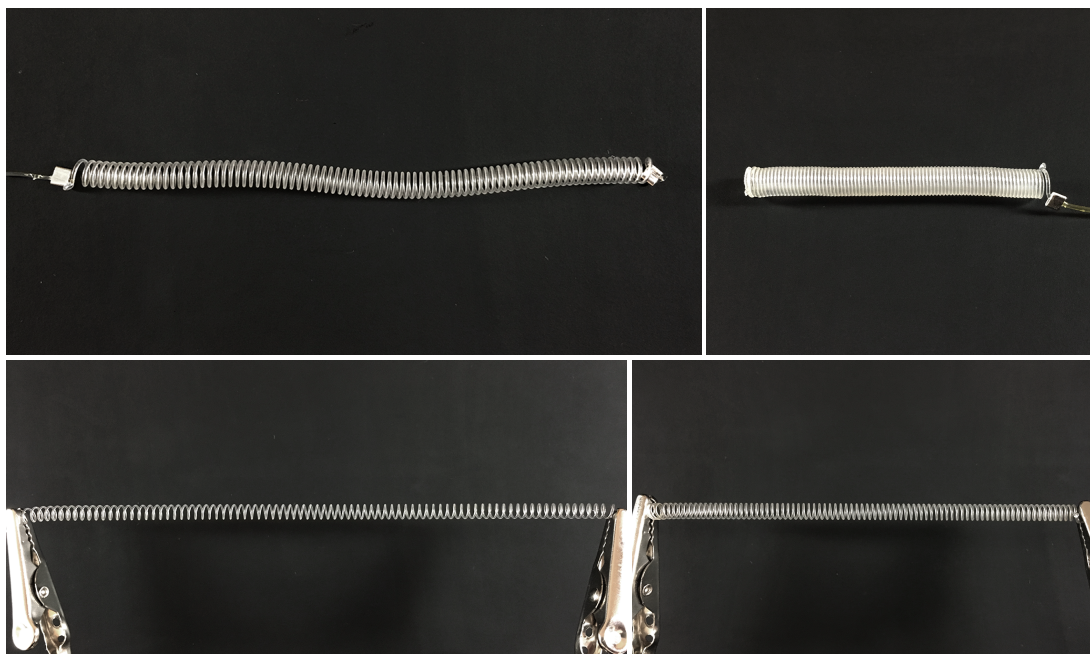


Figure S6. Homochiral (left) and heterochiral (right) mandrel coils heat set at 200°C for 3 minutes. Relaxed coil (top row) and stretched coil (bottom row).

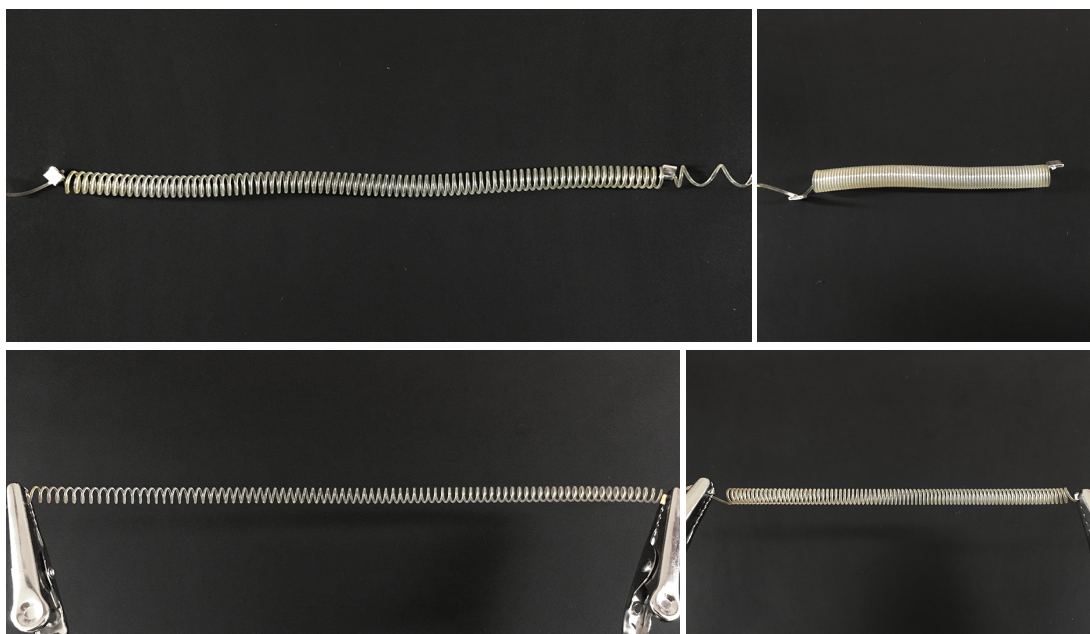


Figure S7. Homochiral (left) and heterochiral (right) mandrel coils heat set at 200°C for 4 minutes. Relaxed coil (top row) and stretched coil (bottom row).

With exposures of 5 and 10 minutes, at 200°C, coils melted during heat setting, resulting either stuck to the mandrel or with adjacent rings stuck to each other (Figure S8 and Figure S9, respectively).

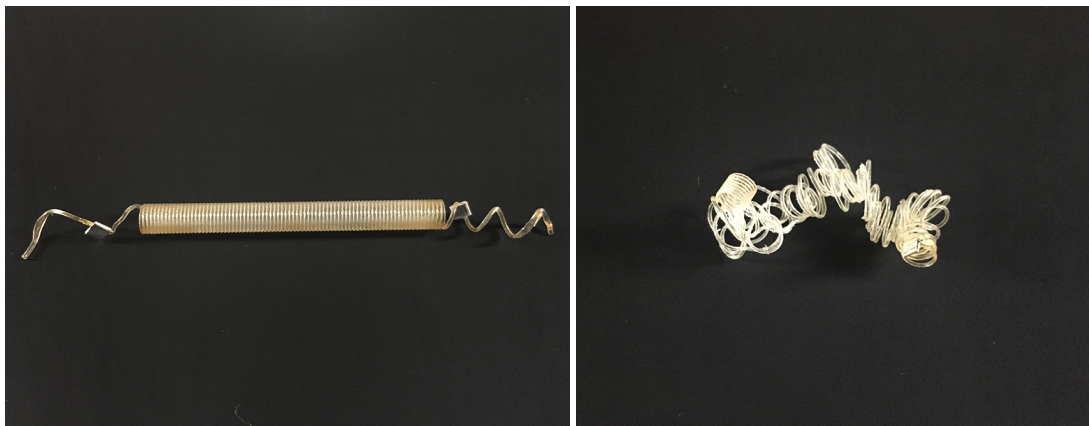


Figure S8. Homochiral (left) and heterochiral (right) mandrel coils heat set at 200°C for 5 minutes.



Figure S9. Homochiral (left) and heterochiral (right) mandrel coils heat set at 200°C for 10 minutes.

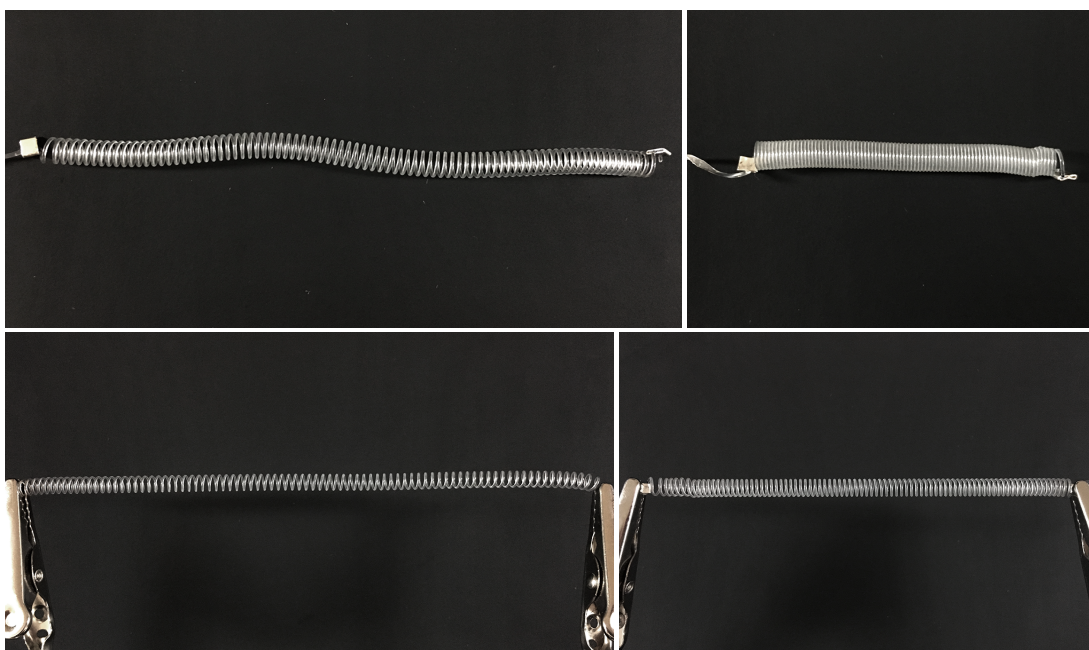


Figure S10. Homochiral (left) and heterochiral (right) mandrel coils heat set at 215°C for 2 minutes. Relaxed coil (top row) and stretched coil (bottom row).

At 215°C with an exposure of 2 minutes, the homochiral coil resulted with separation between adjacent rings, and the heterochiral coil resulted with contiguous rings. Both types of coils did not skew when stretched, and the appearance of the monofilament did not change (Figure S10). The length of both the homochiral and heterochiral coil remained almost constant after 24 hours of removing the samples from the mandrel. Lastly, with an exposure of 3 minutes, at 215°C, samples melted (Figure S11).



Figure S11. Homochiral (left) and heterochiral (right) mandrel coils heat set at 215°C for 3 minutes.

The heat-setting trails presented above, suggest that there might be a threshold in the combination of temperature and exposure time *below* which – when wound with contiguous rings – homochiral coils result with contiguous rings (e.g., samples 27, 42, 29 in Figure S12) and heterochiral coils result with inter-ring separation (e.g., samples 26, 30, 28 in Figure S12); and *above* which homochiral coils result with inter-ring separation (e.g., samples 37, 45, 39 in Figure S12) and heterochiral coils result with contiguous rings (e.g., samples 36, 44, 38 in Figure S12). Furthermore, it seems likely that, at another temperature/exposure time threshold, possibly more intense, the inter-ring separation of homochiral coils starts decreasing (e.g., sample 39 in Figure S12), while heterochiral coils still result with contiguous rings (e.g., sample 38 in Figure S12).

Exposure times longer than 3 minutes at 200°C and 2 minutes at 215°C resulted in the monofilament acquiring a yellow-brown tone or being melted. Given that the length of the coils heat set under 215°C over a 2-minute exposure was considerably stable over time, I decided to use these parameter values to heat set MCs. These heat-setting values provided homochiral coils with separation between adjacent rings, and heterochiral coils with contiguous rings, which, as previously mentioned, are desirable to maximise the amplitude of the shape change when coils are activated from a relaxed, non-stretched nor compressed state.



Figure S12. Heat setting of mandrel coils: Homochiral coils (left) and heterochiral coils (right).

S.1.3. Thermally-induced activation and shape recovery after activation

When thermally activated, the coils formed under the parameter values defined in the previous section, displayed the change in shape at different temperatures. Accordingly, at a given temperature, the amplitude and speed of the expansion or contraction of the coils varied for different samples. Additionally, the ability of the coils to recover their original length, and consequently their original coil pitch, after being heat-activated decreased when samples were activated above a certain temperature, which seemed to be specific (and was unknown) for each sample.

In order to identify a suitable activation temperature for individual samples of heterochiral MCs, without exposing them to the high temperatures that may diminish their ability to recover their length after cooling down, I empirically established a criterion. This criterion takes into account the length of the coil during and after activation (expressed as percentages of the

length of the coil before being activated at the tested temperature) in relation to the activation temperature being tested. The criterion considers that:

If, after being activated at a certain temperature, the length of the coil is *larger than 110%* of its length before being activated at that temperature, then the temperature being tested can be considered a suitable activation temperature for that sample. If the length of the coil after being activated is *smaller than 110%* of its length before activation, then the length of the coil *during* activation should be considered (i.e., the percentage of expansion regarding the length of the coil before activation).

If the length of the coil during activation is *larger than 4 times the value of the tested temperature* (e.g., 160% for an activation temperature of 40°C, or 200% for an activation temperature of 50°C), then the *current temperature* being tested can be considered a suitable one for the activation of that sample. If the length of the coil during activation is *smaller than, or equal to, 4 times the value of the tested activation temperature*, then the activation of the coil should be *tested 10°C above* the current temperature being tested.

I established the criterion by activating samples in hot water, and found 40°C to be a suitable starting temperature to test the activation of the coils formed under the values described in the previous section.⁵ Figure S13 shows a diagram for this criterion, and Figure S14 shows the set-up used to identify a suitable activation temperature for heterochiral MCs.

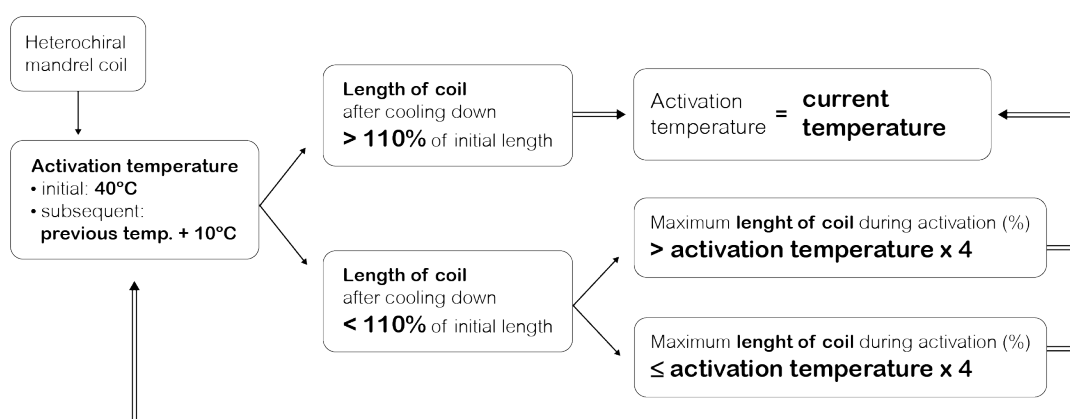


Figure S13. Diagram of the criterion proposed to identify an appropriate activation temperature for individual heterochiral mandrel coils.

⁵ The glass transition temperature (T_g) of nylon is lower in wet conditions than in dry conditions (Hu *et al.*, 2008). Given that the actuation stroke of TCPAs is larger under temperatures above the T_g of the polymer (Haines *et al.*, 2014ab), it can be expected that large expansions take place at lower temperatures in wet conditions than in dry conditions.

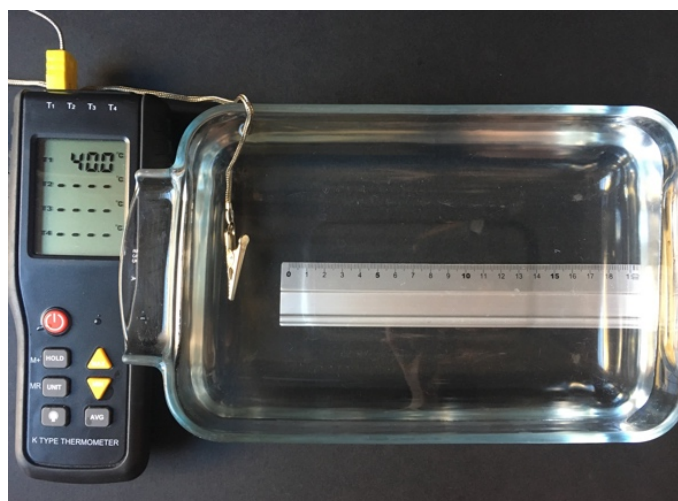


Figure S14. Set-up used in the identification of suitable activation temperatures for heterochiral mandrel coils.

I applied this criterion to a set of 16 heterochiral MCs. These coils were formed from 1.2m monofilament, and after heat setting them their lengths ranged between 4.4cm and 4.7cm. Figure S15 shows the coils before being activated, and Figure S16 shows the coils after being activated.

Samples 22 and 23, fitted the criterion for 40°C and samples 24, 25, 26, 27 and 28 fitted the criterion for 50°C (both groups framed within blue outlines in Figure S16). Nevertheless, these samples were activated at 50°C and 60°C, respectively (i.e., 10°C higher than the activation temperature rated through the established criterion for each group), leading to a substantial increase in their length after cooling down. After being activated at the rated temperature, however, these samples did not completely recover their original length, with lengths after cooling down ranging between 114% and 152% of the initial lengths of the coils, and 104% for one coil (sample 23). Samples 22 and 23 displayed expansions of 158% and 163% of their initial length, respectively; whereas the expansion for samples 24, 25, 26, 27 and 28 ranged between 223% and 261% of the initial length of the coils.

Samples 17, 20, 29, 16, 19, 30 and 31 (framed within orange outlines in Figure S16) were activated only at the rated activation temperature, presenting almost a complete recovery of their length after cooling down. Within this group, samples 16, 19 and 30, displayed expansions between 290% and 301% regarding the initial coil-length at 60°C (rated temperature); sample 17 presented an expansion of 243% at 70°C (rated temperature); and

samples 20 and 29 presented expansions of 355% and 411% respectively during activation at 80°C.

Samples 18 and 21 (framed within the green outline in Figure S16) did not fit the criterion at 50°C, and thus were activated at 60°C, where the recovery of their length diminished. While at 50°C these samples showed smaller expansions than most previously-mentioned samples (i.e., 166% and 191% of the initial length of the coils, respectively), they presented a better recovery of their length at that temperature than at 60°C (100% and 109% of the initial length of the coils, respectively).

By following the proposed criterion, it is possible to identify a suitable activation temperature for individual coils without exposing them to temperatures that are high enough as to diminish their ability to recover their initial length. However, some coils (e.g., sample 18 and 21) might need intermediate activation temperatures, not considered in the current criterion, which is based in temperature increments of 10°C. Thus, smaller temperature increments could be further explored for this criterion.



Figure S15. Heterochiral coils heat set under the defined parameter values, before being activated.



Figure S16. Heterochiral coils after being activated. Suitable activation temperatures identified through the proposed criterion are indicated. Blue outlines show coils that fitted the criterion at the rated activation temperature but, nevertheless, were activated at a temperature 10°C higher than the rated one, showing an increase in their length. Orange outlines show coils that fitted the criterion at the rated activation temperature and have only been activated at that temperature, maintaining their length after being activated or presenting a small increase in length. The green outline shows coils that did not fit the criterion at 50°C, and thus were activated at 60°C, increasing in length.

Once suitable activation temperatures have been identified for a set of coils, these can be trained under these temperatures, and subsequently clustered according to the rated temperatures. Within these clusters, coils can be sub-clustered according to the resulting length of the coil after training, providing groups of samples that will behave in a similar way, i.e., that will present similar expansions at a given temperature.

This criterion represents thus a way of overcoming the variations in the response of heterochiral MCs to heat, which results, most possibly, from variations in the heat-setting process as carried out in this exploration. The criterion allows to stabilise the length, and consequently the pitch of the coils after training, by providing a suitable training temperature without overheating the samples.

In the current stage of formalisation of the formation of homochiral MCs, the pitch with which coils result after heat setting them with the selected values – which is desirable for their activation from a relaxed, non-stretched state – is generally reduced after coils are trained. A similar criterion for the identification of a suitable activation temperature to that established for heterochiral coils can be determined for homochiral ones. Nevertheless, winding them over the mandrel with the desired pitch should be further explored.

The recipe for the formation of MCs, based on the stage of formalisation of the process described here, is included in Appendix C of the main text.

S.2. Tuning of twisted mandrel coils

Twisted mandrel coils (TW-MCs) are formed by inserting twist into a MC and allowing it to fold into itself, forming a snarl, in the same way as twisted twist-induced coils (TW-TICs) are formed (see Appendix B, section B.4.2. of the main text). The structured exploration of this morphological family, beyond identifying suitable values for the formation of samples, focused on understanding the heat-responsive behaviour of different morphological kinds.

S.2.1. Twist insertion and locking of the folded structure

I inserted twist into the MCs using the coiler tool (Figure 41, right-bottom, in the main text), clamping one end of the coil with the jaw of the coiler and holding the opposite end with a plier to prevent it from rotating, in the same way as when forming TW-TICs (Figure 82, left, in Appendix B of the main text). Using the coiler allows to account for the number of turns inserted into the coil. After being folded, these structures should be permanently locked. I used 2mm-diameter metallic crimp tubes to join both ends of the MC, locking only one end of the third-order structure (e.g., Figure S18, Figure S19).

S.2.1.1. Relevant formation parameters

Through the intuitive exploration and the process of translation, I identified the following parameters to be relevant in the formation of TW-MCs (Table 17, main text):

- direction of twisting and winding of the MC (i.e., chirality of the MC);
- MC pitch;
- direction of the inserted twist;
- twist density inserted into the MC;
- activation temperature during training;
- number of training cycles.

Chirality and pitch of the mandrel coil

When considering combinations of both types of MCs (i.e., homochiral and heterochiral ones) and their pitch for the cases of coils with contiguous rings and with separation between

adjacent rings, eight possible cases result, as depicted in the transformations tree (Figure 42 in the main text, and Figure S17).

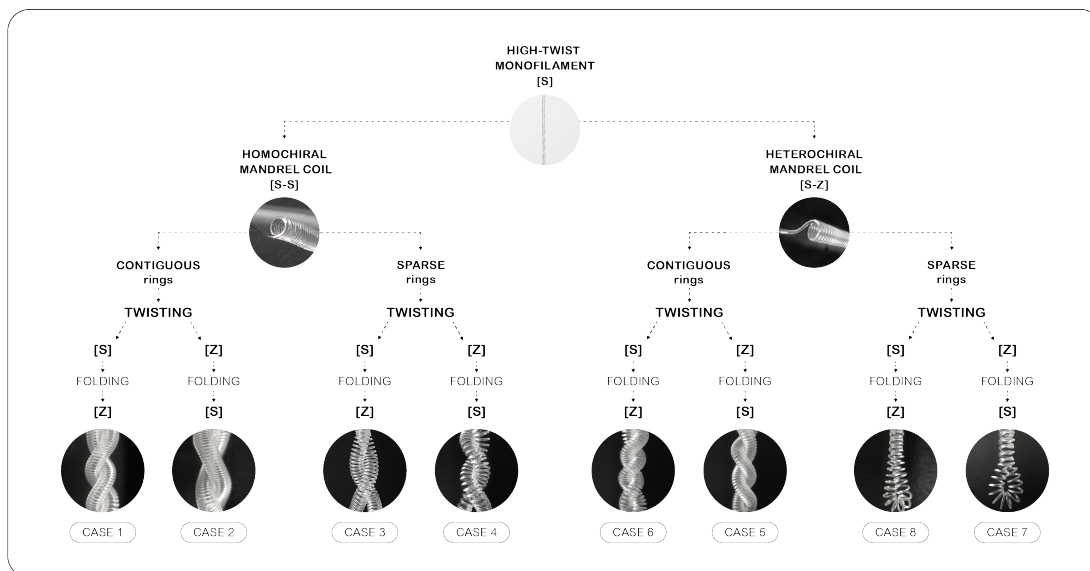


Figure S17. Identification of eight cases for twisted mandrel coils, considering the chirality and the pitch of the mandrel coils.

The separation between adjacent rings of the MC influences the resulting third-order structure once the MCs are folded. For MCs that present contiguous rings, TW-MCs are easily formed (Figure S18). When the distance between adjacent rings is large enough, the two strands of the MC overlap when folded, as can be observed in samples of cases 3, 4, 7 and 8 (Figure S19). When formed from homochiral MCs that have been formed under the values described in the previous section, which result with shorter pitch, individual strands of the MC do not completely merge when folding, as exemplified by samples of cases 3 and 4 (Figure S20).

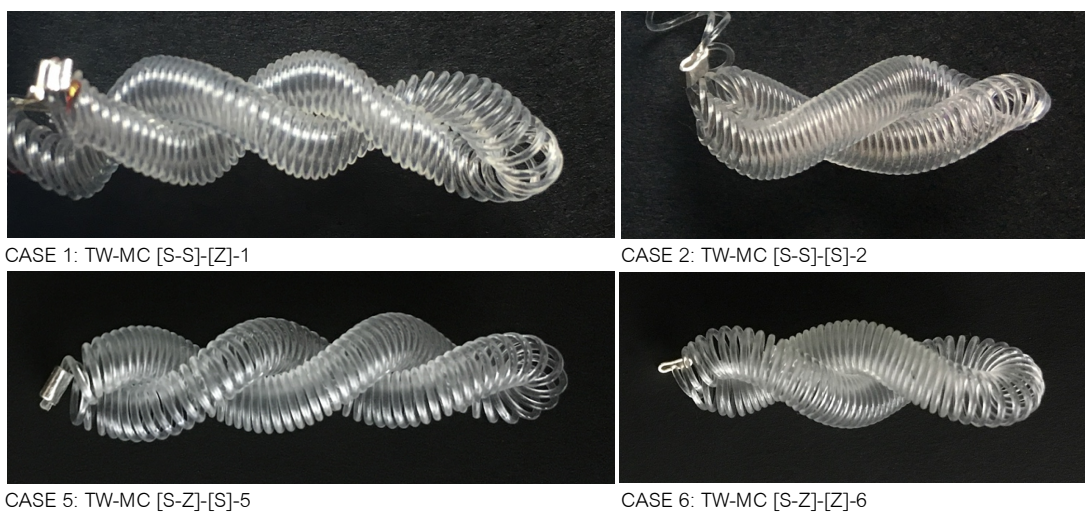
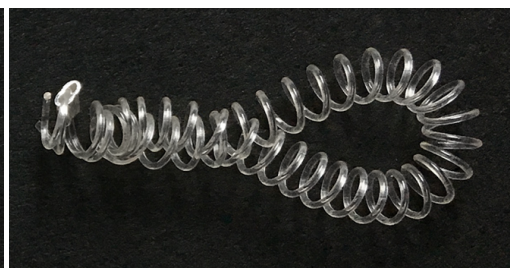


Figure S18. Twisted mandrel coils formed from precursor coils presenting contiguous rings.



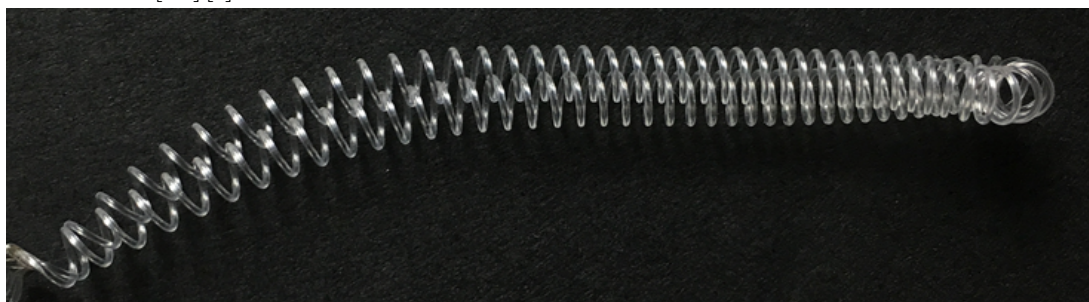
CASE 3: TW-MC [S-S]-[Z]-3



CASE 4: TW-MC [S-S]-[S]-4



CASE 7: TW-MC [S-Z]-[S]-7



CASE 8: TW-MC [S-Z]-[Z]-8

Figure S19. Twisted mandrel coils formed from mandrel coils presenting long pitch.



CASE 3: TW-MC [S-S]-[Z]-3



CASE 4: TW-MC [S-S]-[S]-4

Figure S20. Twisted mandrel coils formed from precursor coils with intermediate pitch.

While I have formed the eight cases for TW-MCs and preliminary described their heat-responsive kinetic behaviour, my focus has been on cases 5 and 6, since these are formed from heterochiral MCs with contiguous rings, for which I have been able to obtain relatively stable structures during this exploration. Moreover, these two cases initially displayed broad and complex heat-responsive behaviours (section 6.2.3 in the main text) which I considered the most appealing.

Number of turns inserted into the mandrel coil

I formed TW-MCs by inserting between 80 turns per meter (t/m; e.g., sample of case 4 in Figure S19) and 477 t/m (e.g., sample of case 1 in Figure S18). In MCs with contiguous rings, when the direction of the inserted twist is opposite to the winding direction of the coil (i.e., cases 2 and 6), after approximately 300 t/m the rings of the MC flip their direction when further twist is added (e.g., Figure S22), as it is described later in the text. In these cases, even after the structure is locked, turns inserted into the second-order structure seem to gather towards the locked end of the TW-MC, diminishing the twist density in the folded structure.

In particular, for cases 5 and 6, through the translation process I found 200 t/m to be a suitable twist density to be inserted into the MC. The twist density in the resulting third-order structure ranged between 50 t/m and 62.5 t/m for samples of case 5 (Figure S21, left column), and between 40 t/m and 65 t/m for samples of case 6 (Figure S21, right column, top three rows).

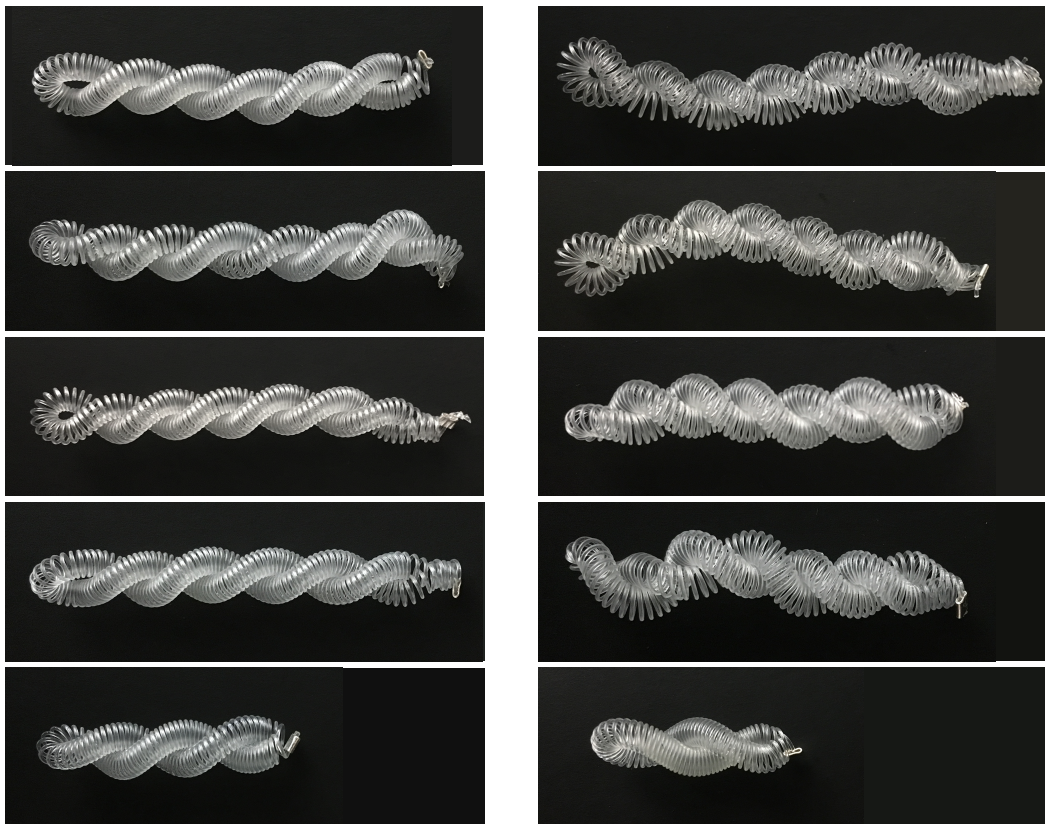


Figure S21. Samples of twisted mandrel coils, case 5 (TW-MC [S-Z]-[S]-5; left column) and case 6 (TW-MC [S-Z]-[Z]-6; right column), formed by inserting 200 t/m into the mandrel coil.

As observed earlier, when the twist inserted into the MC has a direction opposite to the direction of winding of the coil, there seems to be a threshold of twist density after which the

direction of a MC ring flips. If the insertion of twist continues, further rings flip their direction as well, changing the chirality of the coil. Figure S22 (left) shows a homochiral MC whose rings have been made to flip their direction (right side of the coil). When the insertion of twist is done without stretching the coil, the original pitch of the MC remains unchanged (e.g., Figure S22, right), whereas if the MC is stretched while inserting the twist, the area that changes chirality will present a larger pitch (e.g., Figure S22, left). Furthermore, the two areas of the coil (i.e., the one with the original and the new chirality) may adopt a perpendicular orientation to each other, enabling to form three dimensional shapes with the MC, as seen in Figure S22, right. These features can be exploited, for example, by selectively shifting the chirality of a heterochiral MC with contiguous rings, into areas of homochiral coil with larger pitch (by inserting twist into the coil while stretching it), thus obtaining one same sample that will expand and contract in the respective areas.

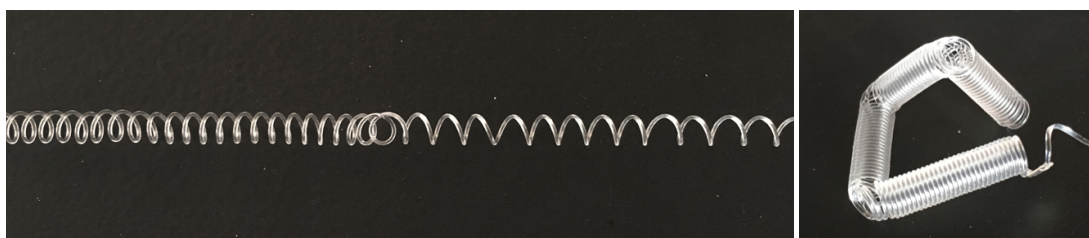


Figure S22. Homochiral mandrel coil whose chirality has been changed by inserting a twist to the stretched mandrel coil, with a direction opposite to the direction of winding of the coil (left). Heterochiral mandrel coil with contiguous rings, whose chirality has been changed in certain areas, forming a three-dimensional structure (right).

S.2.2. Training of twisted mandrel coils

TW-MCs should ideally be formed from MCs that have been previously trained, as described in section S.1. However, samples formed during this exploration employed MCs that have not been previously heat-activated. In this case, TW-MCs do not seem to lose third-order turns when being activated repeatedly, but in some cases, they do change in length and pitch of the second-order MC, possibly when the activation temperature used was not an appropriate one, as described earlier for heterochiral MCs.

S.2.3. Heat-responsive kinetic capacity of twisted mandrel coils

When considering the activation of TW-MCs from a relaxed, non-stretched nor compressed state, structures formed from homochiral MCs with contiguous rings (i.e., cases 1 and 2, Figure S18, top row) do not display any readily visible change in shape in response to heat: given that adjacent MC rings are already in contact, there is no space for the contraction to take place.

Cases 3 and 4, display small changes in shape, even when they are formed from MCs with long pitch, as the samples shown in Figure S19. When activated in a hot plate (set-up 5, described in Table 9 in the main text and section B.5.2 of Appendix B), this sample of case 3 rolled over the hot surface while contracting, stopping and slightly lifting both ends when adjacent rings got closer together, to then fall towards the opposite direction in which it was rolling (Figure S23). The sample of case 4 bended upwards while contracting until adjacent rings touch each other (Figure S24). For both structures, the shape change stopped once adjacent rings came into contact.

When activated with hot air under set-up 1 (described in Table 9 in the main text and section B.5.2 of Appendix B; Figure S25), samples of cases 3 and 4 formed from MCs with intermediate pitch, as the ones shown in Figure S20, contracted while slightly untwisting. The heat-responsive shape change of these structures tends to become smaller when formed from the homochiral MCs resulting from this exploration, given that the latter tend to diminish their pitch during training, as mentioned in section S.1.

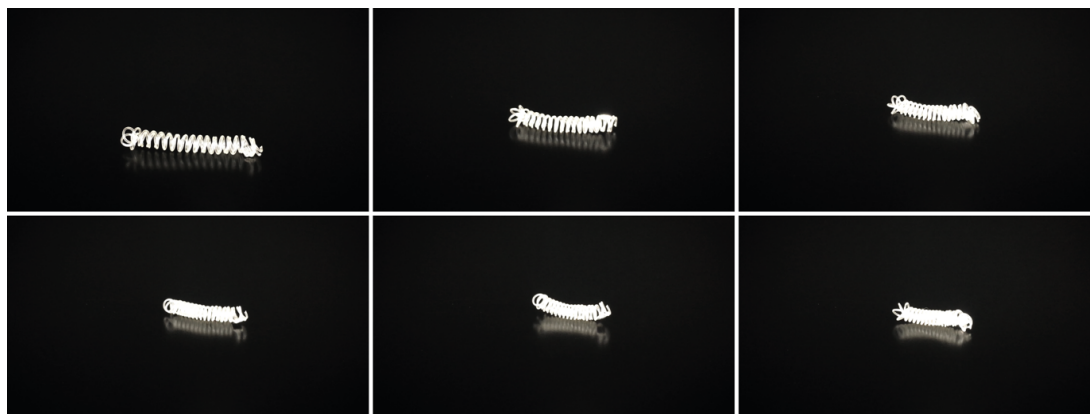


Figure S23. Activation of a twisted mandrel coil, case 3 (TW-MC [S-S]-[Z]-3), on a hot plate.

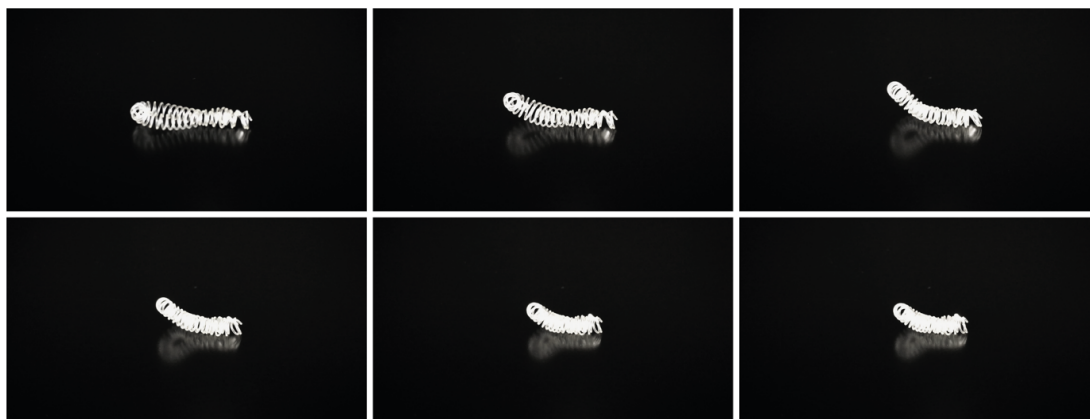


Figure S24. Activation of a twisted mandrel coil, case 4 (TW-MC [S-S]-[S]-4), on a hot plate.



Figure S25. Activation of twisted mandrel coils, cases 3 (TW-MC [S-S]-[Z]-3) and 4 (TW-MC [S-S]-[S]-4), under hot air (left and right sequence, respectively). For both samples: initial shape (left), maximum shape change during activation (centre) and shape after cooling down (right).

Samples of cases 5 and 6, being formed from heterochiral MCs with contiguous rings, expand in response to heat. Together with this expansion, a slight further twisting is also visible when samples are activated with hot air under set-up 1 (Table 9 in the main text and section B.5.2 of Appendix B; Figure S26, clip-charts 16, 17, 18, 19). When samples reach a certain degree of expansion, and adjacent second-order rings acquire enough separation between them, both strands of the TW-MC overlap (e.g., Figure S27). When this happens, the folded third-order structure needs to be manually restored after the sample has cooled down.

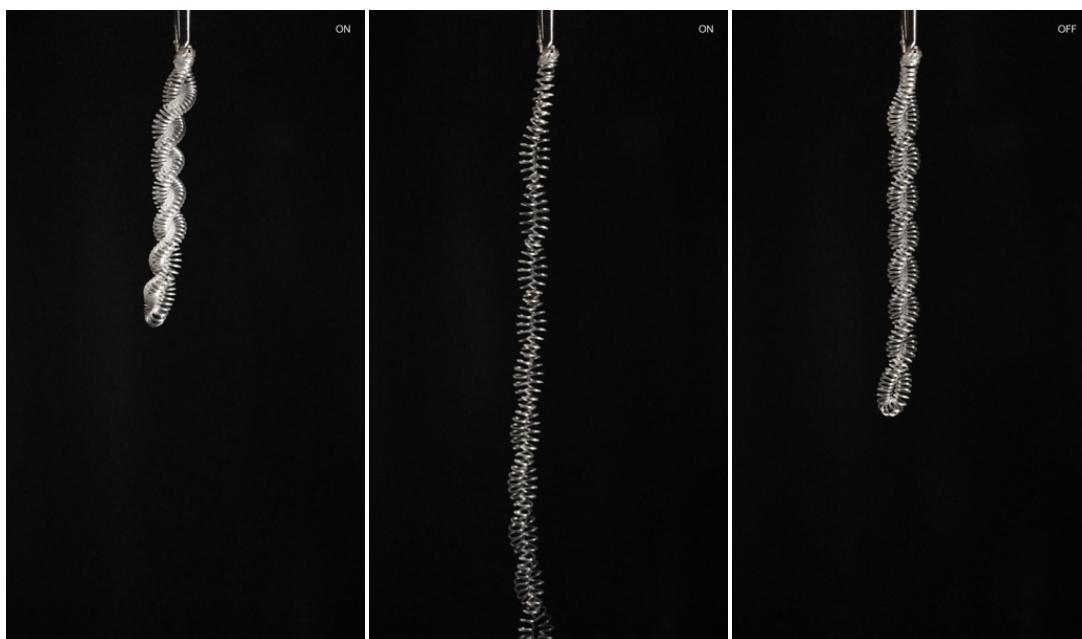
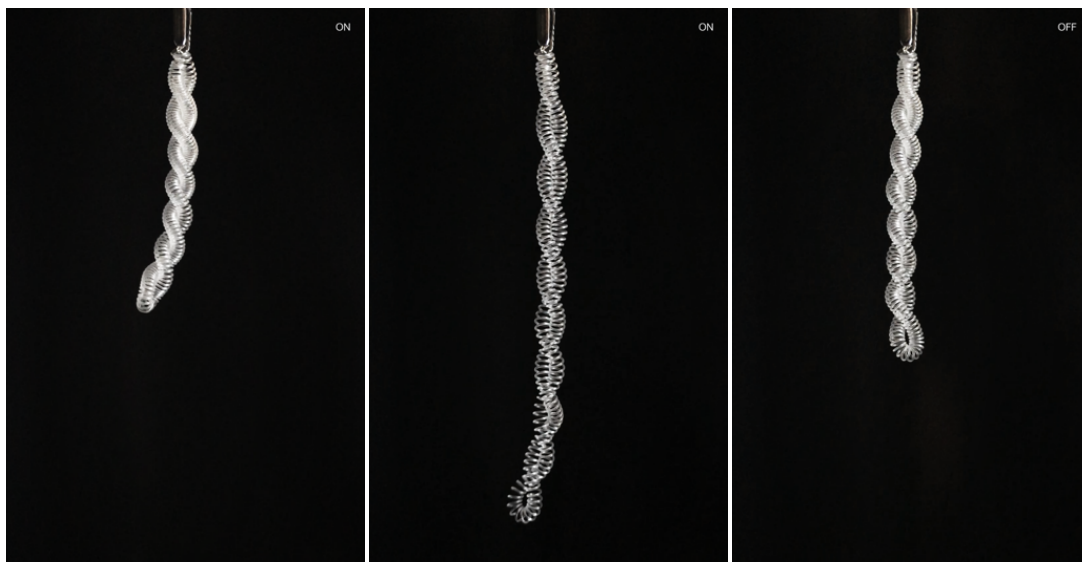


Figure S26. Activation of twisted mandrel coils, cases 5 (TW-MC [S-Z]-[S]-5) and 6 (TW-MC [S-Z]-[Z]-6), with hot air (top and bottom sequence, respectively). For both samples: initial shape (left), maximum shape change (centre) and shape after cooling down (right). See clip-charts 16, 17, 18, 19.



Figure S27. Activation of a twisted mandrel coil, case 5 (TW-MC [S-Z]-[S]-5), with hot air: initial shape (left), maximum shape change (centre) and shape after cooling down (right). The strands of the TW-MC overlap when the second-order structure reaches a certain degree of expansion.

Comparing the heat-responsive behaviour of TW-MCs cases 3 and 4 with that of cases 5 and 6, it seems that these structures do not follow the same principle as TW-TICs do, by which third-order structures whose direction matches the direction of the second-order coil (i.e., TW-TIC[S-S]-[S]) untwist in response to heat when activated with at least one end loose; and those in which these directions are opposite (i.e., TW-TIC[S-S]-[Z]) twist further in response to heat under such arrangement (see Table 1 in the main text). TW-MCs cases 3 and 4 are formed from MC[S-S] and the third-order structure in case 3 follows the Z direction, whereas in case 4 it follows the S direction. Nevertheless, together with a small contraction, both these structures slightly untwist in response to heat,⁶ with this untwisting taking place towards opposite directions for each case. Cases 5 and 6 are formed from MC[S-Z] and the third-order structure in case 5 follows the S direction, whereas in case 6 it follows the Z direction. However, together with a rather large expansion, both these structures slightly twist further in response to heat, and this twisting further takes place towards opposite directions in each structure. Comparing these two pairs of cases, it seems that the untwisting and twisting further behaviours of the third-order structure in TW-MCs is determined by the chirality of the second-order MC itself, rather than by the relative directions of the second and third structural levels.

When activated in a hot plate, cases 5 and 6 roll laterally over the hot surface while expanding, performing large displacements. The qualities of this rolling vary across samples, in some cases being generally smooth and continuous with eventual changes in acceleration and speed (e.g., TW-MC[S-Z]-[S]-5-2m, TW-MC[S-Z]-[Z]-6-1m and TW-MC[S-Z]-[Z]-6-2m, clip-charts 17, 18 and 19, respectively) and in other case being jagged and intermittent, advancing with sudden dislocations through changes in acceleration (e.g., TW-MC[S-Z]-[S]-5-1m, clip-chart 16). Spontaneous changes in the direction in which the sample displaces itself over the hot surface also take place (e.g., TW-MC[S-Z]-[S]-5-2m, clip-chart 17).

The behaviour displayed by samples 19 and 20, introduced in Chapter 6 of the main text (Figures 22, 23 and 21) and corresponding to TW-MC[S-Z]-[S]-5 and TW-MC[S-Z]-[Z]-6, respectively, was not displayed by the samples formed during this structured exploration. This might be due to the use of lower temperatures in the hot surface, since not all samples

⁶ It is possible that the untwisting effect in cases 3 and 4 results from the shortening of the length of the third-order structure.

reach an expansion that is large enough as to allow the two strands of the TW-MC to overlap and acquire the “loop and tail” configuration observed for samples 19 and 20 acquired, and which may be enabling this particular behaviour. In the case when the overlapping of the two strands did take place during the present exploration (e.g., TW-MC[S-Z]-[S]-5-2m, clip-chart 17), the size of the loop was relatively small in comparison with the size of the “tail”, which together with the longer length of the sample might be preventing the “tail” passing through the loop, as observed in samples 19 and 20.

Samples of cases 7 and 8, being formed from heterochiral MCs, also expand in response to heat; but since the precursor MCs already presented a distance between consecutive rings, the expansion effect was limited. While a torsional behaviour cannot be readily observed under single anchoring arrangements (e.g., activation set-up 1, as described in Table 9 in the main text and section B.5.2 of Appendix B), when activated on a hot plate (activation set-up 5), both samples rolled over the hot surface while expanding, suggesting such a torsional movement (Figure S28 and Figure S29; clip-charts 20 and 21, respectively). Changes in the direction in which the sample displaces itself while rolling also took place for case 7.

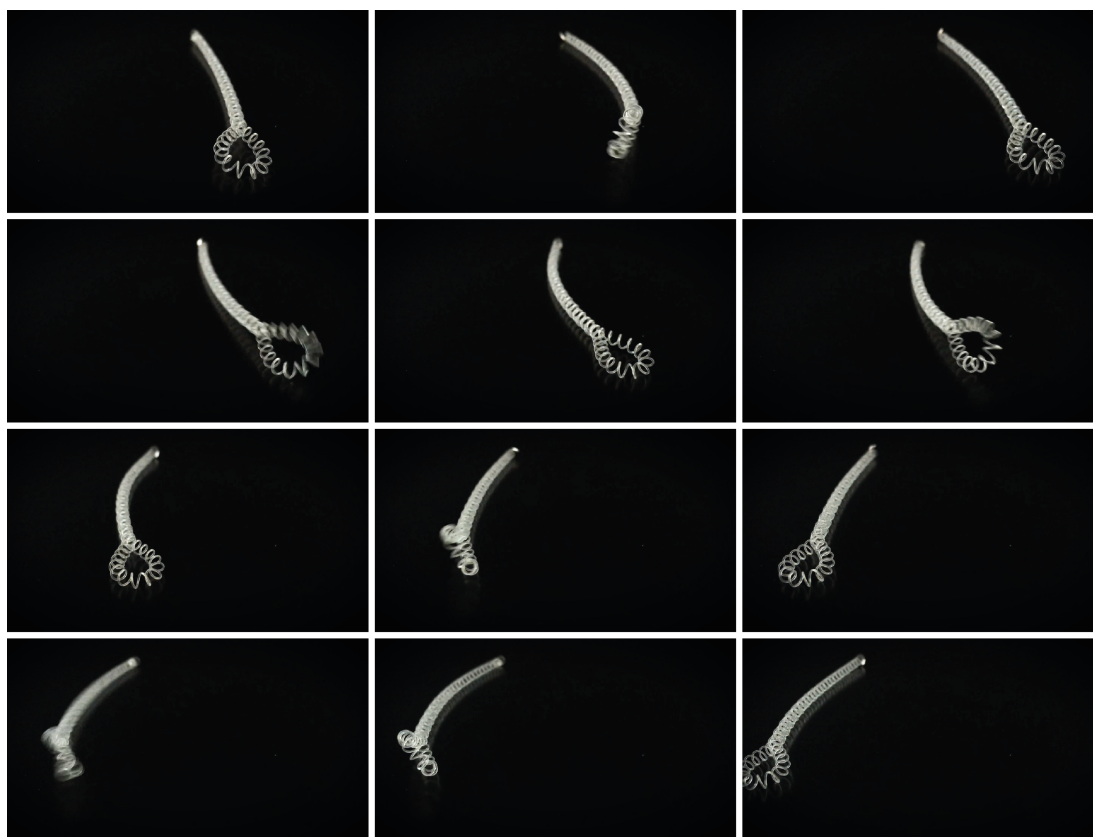


Figure S28. Activation of a twisted mandrel coil, case 7 (TW-MC [S-Z]-[S]-7), on a hot plate (clip-chart 20).

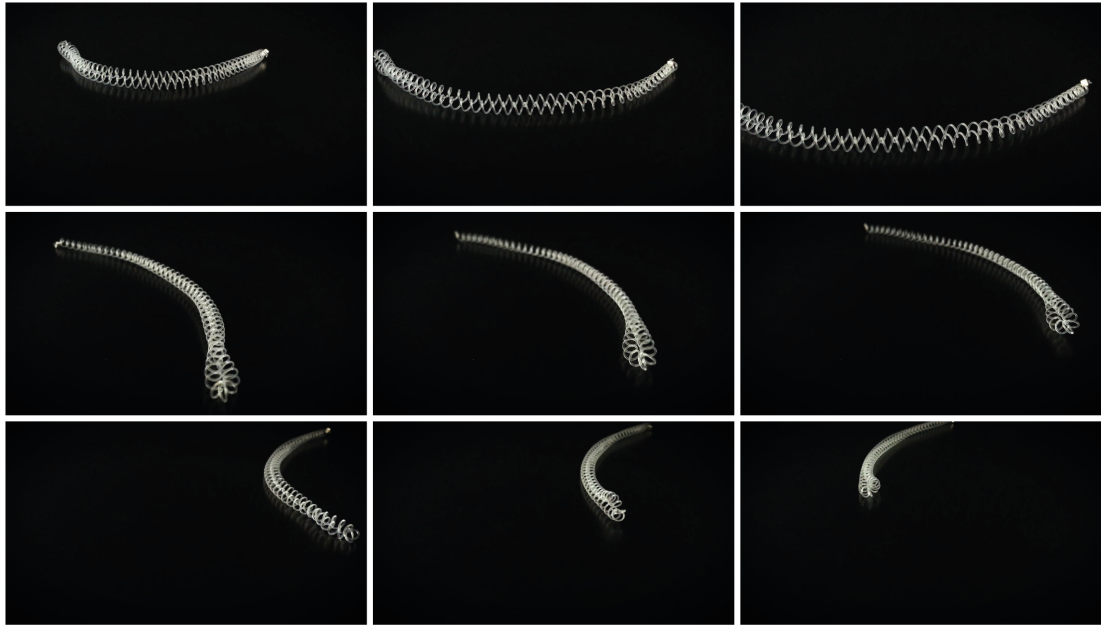


Figure S29. Activation of a twisted mandrel coil, case 8 (TW-MC [S-Z]-[Z]-8), on a hot plate (clip-chart 21).

References

- Haines, C. S., Li, N., Spinks, G. M., Aliev, A. E., Di, J., Baughman, R. H. (2016) New twist on artificial muscles. In *Proceedings of the National Academy of Sciences*. **113**(42), pp.11709–11716. doi: 10.1073/pnas.1605273113.
- Haines, C. S., Lima, M. D., Li, N., Spinks, G. M., Foroughi, J., Madden, J. D. W., Kim, S. H., Fang, S., De Andrade, M. J., Göktepe, F., Göktepe, Ö., Mirvakili, S. M., Naficy, S., Lepró, X., Oh, J., Kozlov, M. E., Kim, S. J., Xu, X., Swedlove, B. J., Wallace, G. G., Baughman, R. H. (2014a) Artificial muscles from fishing line and sewing thread. *Science*. **343**(6173), pp.868–872. doi:10.1126/science.1246906.
- Hu, J., Dong, Z., Liu, Y. and Liu, Y. (2008) The Investigation about the Shape Memory Behavior of Wool, *Advances in Science and Technology*, 60, pp.1–10. doi: 10.4028/www.scientific.net/AST.60.1.
- Wypych, G. (2016) *Handbook of Polymers*. 2nd edn, *Handbook of Polymers*. Second edn. ChemTec Publishing. doi: 10.1016/C2015-0-01462-9.